



Contents lists available at <http://qu.edu.iq>

## Al-Qadisiyah Journal for Engineering Sciences

Journal homepage: <https://qjes.qu.edu.iq>



# Improving the efficiency of the automobile engine cooling system using hybrid MWCNT/Al<sub>2</sub>O<sub>3</sub> as nanofluids

Ahmed A. Mohammed\*<sup>1</sup> , H. I. Dawood<sup>1</sup> , and Helen N. Onyeaka<sup>2</sup> 

<sup>1</sup>Department of Chemical Engineering, Faculty of Engineering, University of Al-Qadisiyah, Al-Diwaniya 58002, Iraq

<sup>2</sup>School of Chemical Engineering, University of Birmingham, Birmingham, UK.

### ARTICLE INFO

#### Article history:

Received 14 November 2023

Received in revised form 27 December 2023

Accepted 15 March 2024

#### Keywords:

Radiator

Nanofluid

Heat Transfer

Automotive engine

Thermal conductivity

### ABSTRACT

The aim of this research was to increase the engine car efficiency by adding an innovative material called hybrid MWCNT/Al<sub>2</sub>O<sub>3</sub> nanofluids. A volume ratio instance for investigations is 0.05 MWCNT mixed with 0.05 Al<sub>2</sub>O<sub>3</sub> in distilled water (DW). The experimental temperature setup was in the range from 50 °C to 70 °C. The results demonstrate that as temperatures increase, specific heat and thermal conductivity increase significantly, while viscosity and density gradually decrease. At 70 °C, the highest thermal conductivity of 1.143 W/m.K was achieved in the presence of hybrid MWCNT/Al<sub>2</sub>O<sub>3</sub> nanofluids. Furthermore, it was found that the correlation coefficient for thermal conductivity is 97.06% R<sup>2</sup>.

© 2024 University of Al-Qadisiyah. All rights reserved.

## 1. Introduction

The Kyoto Protocol, which was introduced in 1997, had the noble intention of tackling the problem of greenhouse gas emissions [1]. Countless studies have been dedicated to discovering alternative methods of combating the harmful exhaust emissions produced by vehicles. The release of noxious gases from car engines is a major contributor to the alarming issue of global warming. One promising strategy involves improving the cooling system of the engine, which has the potential to decrease energy usage. The process of heat transfer is pivotal in both industrial and consumer goods alike. It is of utmost importance to make sure that the temperature of the engine stays within the ideal range of 90 °C to 105 °C. This helps prevent any damage to the engine and also enhances fuel efficiency and lubrication [2]. Cooling the engine is a big challenge

faced by different industries such as manufacturing, electrical, and automotive sectors. Many cooling systems used in industries and automobiles are currently struggling with this problem.

Utilizing traditional cooling agents like water, motor oils, and optoelectronic systems, various industries including air-conditioning, power generation, and chemical processes employ ethylene glycol-processing instruments, mineral oil, and other sectors [3].

Unfortunately, it has been discovered that conventional coolants like engine oil and ethylene glycol are not as efficient as desired. In order to address this issue, there is a pressing requirement for a more effective fluid that has exceptional heat transfer abilities. This is where nanofluid comes into the picture - an advanced technology that blends base fluids with nanoparticles

\* Corresponding author.

E-mail address: [eng.chem21.post4@qu.edu.iq](mailto:eng.chem21.post4@qu.edu.iq) (Ahmed A. Mohammed)

<https://doi.org/10.30772/qjes.2023.144421.1047>

2411-7773/© 2024 University of Al-Qadisiyah. All rights reserved.



This work is licensed under the [Creative Commons Attribution 4.0 International License](https://creativecommons.org/licenses/by/4.0/).

to improve heat transfer in heat exchangers. Extensive research studies have been conducted to examine the thermal properties and heat transfer efficiency of Al<sub>2</sub>O<sub>3</sub>-MWCNT when combined with different base fluids, including water [4].

Ever since nanofluid applications were introduced, researchers have been increasingly interested in exploring their potential [5-9]. It has become imperative to develop new technologies that can enhance modern automobile technology in a more efficient and environmentally friendly manner [10]. Unfortunately, it has become a common occurrence for vehicles to experience breakdowns on the side of the road due to issues with overheating. The primary causes of engine overheating are a deteriorating water pump, a worn-out radiator, and inefficient coolant. This can result in various damages, such as warped cylinder heads, distorted radiator hoses, and ultimately, a complete breakdown of the car [11]. Though there is ample space for enhancement, we have a variety of options at our disposal. One way to improve the car's cooling system is by making it more efficient. This can be accomplished through passive cooling, active cooling, or a blend of both techniques [12]. It is crucial to keep the engine's temperature in check to avoid any mechanical issues due to overheating while also ensuring optimal fuel consumption and preventing excessive cooling. In recent times, scholars have dedicated their efforts to improving the thermal efficiency of radiators to foster environmental sustainability. One method that has proven to be effective is using cooling fluids that have better thermophysical properties. However, this approach often requires the use of external power sources to improve the cooling capabilities. For example, one can install a cooling fan to eliminate extra heat or introduce an antifreeze solution, which is a combination of water and antifreeze. This information is mentioned in reference [13].

In this research paper, a groundbreaking technology is introduced: the utilization of a hybrid nanofluid to enhance the physical properties in contrast to a standard fluid. To create this suspension, ultrasonic waves were employed, resulting in nanoparticles ranging from 1 to 100 nanometres in size. Table 1 showcases the diverse range of nanoparticles that can be utilized, including metal oxides, metal carbides, ceramics, minerals, and metal nitrides. These particles have the remarkable ability to significantly enhance heat transfer in coolants when compared to traditional fluids, even at low concentrations. A concentration as minimal as [14] can yield a remarkable improvement of over 50% in heat transfer for current applications.

**Table 1.** Nanoparticles materials.

Minerals	Gold, copper
Metal oxide	Alumina, silicon oxide, zirconium oxide, titanium oxide
Oxide ceramics	Al <sub>2</sub> O <sub>3</sub> , CuO, TiO <sub>2</sub>
metal carbide	silicon carbide
various forms of carbon	Carbon nanotubes, diamond, graphite
metal nitride	Ain, Sin

## 2. Materials

This study utilized two different types of nanoparticles, specifically Al<sub>2</sub>O<sub>3</sub> nanoparticles obtained from Hongwu, China and Universal Group Ltd., as well as MWCNT obtained from Cheap Tube Inc. in the USA. The suspension of nanoparticles in deionized water (DW) was achieved using a two-step procedure, with the aim of developing a foundation coolant.

Furthermore, Table 2 provides a description of some additional characteristics shown by these nanocomposites.

**Table 2.** Main properties of DW, Al<sub>2</sub>O<sub>3</sub> and MWCNT nanoparticles.

Properties	DW	(Al <sub>2</sub> O <sub>3</sub> )	MWCNT
Color	colorless	White	black
Size of the particle (nm)	-----	44.7	20-40
Pureness of particle (%)	-----	99.99	98.7
The particles shape	-----	Spherical	Tube
Exterior	liquid	Powder	Powder
Density (g.cm <sup>-3</sup> )	0.998	3.9	2.1
Thermal conductivity (K) (W.m <sup>-1</sup> . K <sup>-1</sup> )	0.6	40	3000
Specific heat (cp) (J / kg. k)	4179.6	773	769

## 3. Experimental design

The experimental setup utilized in the investigation is schematically diagrammed in Fig. 1, which also offers a broad overview of the apparatus's component pieces.

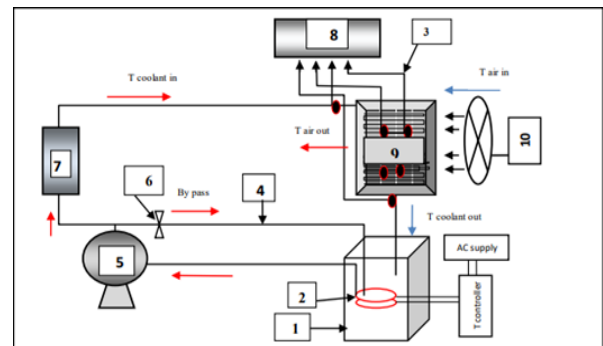


**Figure 1.** Diagrammatic schematic of the test apparatus [15].

The basic elements of the experimental system are as follows:

- The reservoir is made of iron and has an extended fiberglass protection plate covering it. The thickness of this plate is roughly 8 mm. The container's precise measurements are L = 530 mm, W = 150 mm, and H = 700 mm.
- Heating:** Custom piping is the component of the heater that heats the water. It is a coil with a temperature-sensing component (accuracy  $\pm 1$ ) that controls the medium's temperature to a specific degree.
- Thermocouples:** Let's take a closer look at coolant temperature assessment. What we are talking about here is the use of 8 "Type K Thermocouples". Yes, directly from Shanghai; the model number is WRN-131, accuracy is  $\pm 0.1$ . These bad boys can withstand temperatures ranging from  $-270^{\circ}\text{C}$  to  $1260^{\circ}\text{C}$ ! Two of them are now connected to our ductwork - so they can directly measure the temperature difference between the cooler inlet and outlet. We then installed six more on each side of the radiator - very handy stuff.

- d) Flow line: plastic pipe made of polypropylene with a diameter of approximately 25 mm and covered with fiberglass insulation. Its length is approximately 3 m, which controls the volume of liquid in the circuit.
- e) Pump: A water pump (Pedrollo, PKM80, Italy) was employed to pump the fluid through the flow path.
- f) **Valve:** Polypropylene gate valve for regulating the flow of the working medium.
- g) **Flow meter:** In our cooler experiment, we measured the coolant flow rate using an American Instruments, Panel, LZTM-15 temperature measuring device. This device can withstand temperatures of up to 100 degrees Celsius and has an accuracy of just around 0.5%, which is incredible.
- h) Data Acquisition System: The system displays the data logger (iron, dimensions L = 450, W = 500, H = 150), which has a  $\pm 0.5\%$  accuracy for all thermocouples.
- i) Radiator: This investigation utilized an automotive radiator, a heat exchanger that crosses itself. The radiator of the Toyota Corolla (China, Jinan Jiada International Trade Co., Ltd.) has a capacity of 2 litres. Automotive radiators employ finned sections and vertical aluminum tubes with a flat profile.
- j) Forced draft fan: 1000-rpm fan (China, BORK, APG-20) near the outer wall of the radiator. Includes a controller that controls the fan speed. The speed was designated as 1000 revolutions per minute in this investigation.

#### 4. Nanofluid preparation

Utilizing the sensitive balance, the requisite weights for every MWCNT and Al<sub>2</sub>O<sub>3</sub> were measured. Precise measurements of nanoparticle weights were taken utilizing the German Sartorius sensitive balance (TE 214S, maximum weight 210 g). The nanofluid was given a capacity of 10 liters, of which half were set aside to hold the weight that was being measured. The suspensions of nanoparticles in distilled water were subjected to an ultrasonic vibration for three hours to examine the impact of the sonication time on the stability of the nanofluid. The samples were then treated with ultrasonic waves for a further hour at room temperature. Before this, 500 milliliters of distilled water were added to the weights that had previously been measured. The thermal characteristics and heat-transfer capacities of Al<sub>2</sub>O<sub>3</sub>-MWCNT have been studied in the past in a variety of base fluids, including water [16].

To efficiently prepare the suspended fluids, the GT SONIC T-Series Ultrasonic Cleaner, manufactured in China, was used. The following equation [17] is used to get the volume concentrations of single and hybrid nanofluids.

$$\text{Volume concentration } (\varphi) = \left[ \frac{\frac{W_{np}}{\rho_{np}}}{\frac{W_{np}}{\rho_{np}} + \frac{W_{bf}}{\rho_{bf}}} \right] * 100 \quad (1)$$

Where  $\rho_{bf}$  represents the density of the DW in  $\text{g.cm}^{-3}$  and  $W_{bf}$  represents the weight in g of the DW and the weight in g of the nanoparticles and  $\rho_{np}$  the densities in  $\text{g.cm}^{-3}$  of the particles.

#### 5. Experimental data analysis

The procedures followed during the experimental research will be highlighted in this section. The sample was first put inside the experimental system's tank, and then the temperature and volume flow rate were adjusted to 50 °C and 3 LPM, respectively. The temperatures of the radiator's front and rear walls, as well as the intake and exit of the nanofluid, had to be noted. Multiple experiments with different variable adjustments and recording of the outcomes were then required.

#### 6. Data extraction

The thermal characteristics of distilled water were evaluated at 50, 60, and 70 °C using a thermodynamic chart [18]. It was possible to approximate these thermal properties by using nanofluids to estimate viscosity, specific heat, density, and thermal conductivity. The size of the nanoparticles has no discernible impact on the thermal conductivity of the fluid, according to a recent review of research [19] on alumina nanofluids. Through the use of Hamilton and Crosser Eq. 2, the thermal conductivity of the nanofluid was ascertained [7]. Using Einstein's equation (3), the viscosity of the nanofluids was determined [20]. Using the related Eqs. 4 and 5, the specific heat and density of the nanofluids were then calculated [21].

$$K_{nf} = \frac{K_p + (n-1)K_{bf} + (n-1)(K_p + K_{bf})\varphi}{K_p + (n-1)K_{bf} - (K_p + K_{bf})\varphi} * K_{bf} \quad (2)$$

$$\mu_{nf} = (1 - 2.5\varphi_p) \mu_{bf} \quad (3)$$

$$\rho_{nf} = (1 - \varphi) \rho_{bf} + \varphi \rho_p \quad (4)$$

$$Cp_{nf} = (1 - \varphi) Cp_{bf} + \varphi Cp_p \quad (5)$$

( $\varphi$ ) is the unit of measurement for nanoparticles per unit volume. The abbreviations nf, bf, and p stand for nanofluids, basic fluids, and particles, respectively. The units of measurement for viscosity, density, and specific heat are  $\mu$  in mpa.s,  $\rho$  in  $\text{g/cm}^3$ , K in (W/m.K), and Cp in J/kgK..

#### 7. Results and discussions

This study made sure that the data were precisely aligned and that the model was accurate by using the Minitab 17 software's response surface analysis of variance (DOE) technique. An experimental system with different input temperatures and flow rates was used to collect data on nanofluid performance. The results showed that temperature had an effect on the physical characteristics of nanofluids, including density, viscosity, specific heat capacity, and thermal conductivity. As the temperature rose, unexpected consequences were seen. As noted in [22], it is important to remember that going too far into the thermal properties of nanofluids might result in

catastrophic accidents. In particular, the physical characteristics of a sample were investigated in this study between 30 and 70 degrees Celsius.

**7.1. Thermal conductivity**

In the analysis results depicted in Fig. 2, the temperature values are graphed against the thermal conductivity of both the base fluid and all nanofluids. The experiments primarily focused on a volume fraction of 0.05 MWCNT-0.05 Al2O3 and utilized a temperature range spanning 3 degrees. This figure showcases a clear correlation between rising temperature and increasing thermal conductivity within the nanofluid. Interestingly, this finding aligns with a previous study [23], which proposed that the movement of nanoparticles within a liquid environment intensifies as the temperature climbs. It was Xu and Roetzel [24] who originally uncovered that Brownian motion can weaken molecular bonds, thus lending support to this intriguing phenomenon. It is quite fascinating to observe that the data unambiguously demonstrate a notable increase in the thermal conductivity of the nanofluid, in comparison to distilled water (DW). To illustrate, while DW exhibits a mere thermal conductivity of 0.6 W/m.K at temperatures up to 70 °C, the (MWCNT/Al2O3) nanofluid boasts a thermal conductivity of 1.143 W/m.K. In their research, Kumar and Sarkar [25] experimented to gauge the thermal conductivity of the Al2O3-MWCNT/water mixed nanofluid by manipulating the ratio. At a temperature of 30 °C, the combination of Al2O3 and MWCNT at a ratio of 1:4 yielded a thermal conductivity (TC) value of 0.6195 W/mK, as reported by the researchers. By examining the relationship between operational variables and practical parameters, and applying the mathematical correlation derived from Equation 6, it is possible to make predictions about thermal conductivity using experimental data. The Eq. 6 is used for regression analysis. Table 3 shows the high value of R^2 (97.10%),

**7.2. Density**

The density of the nanofluid is dependent on both the base fluid's density and the presence of nanoparticles. The base fluid's density rises as a result of the nanoparticles' solid state. As Figure 3 illustrates, the density of nanofluids is higher than that of distilled water and falls with temperature. For instance, distilled water has a density of 0.993 g/cm3, whereas the density of nanofluids at 50°C is 1.194 g/cm3. The density of distilled water drops to 0.983 g/cm3 while the density of nanofluid drops to 1.185 g/cm3 when the temperature rises to 70°C. According to the mathematical correlation, density from experimental data can be predicted by looking at the correlations between operating factors in terms of useful parameters Eq. 7. Table 4 shows the high value of the R^2 (97.06%) that the model delivers a good fit to the data.

**7.3 Specific heat of nanofluid**

In Fig.e 4, we can observe the specific heat of different samples at various temperatures. The specific heat of nanofluids is influenced by multiple factors, including the type of base fluid and the nanoparticles present in it, among other physical parameters. It is important to note that DW exhibits a notably higher specific heat compared to the other samples.

**Table 3.** Summary of thermal conductivity regression coefficient model.

S	R-sq	R-sq(adj)	R-sq(pred)
0.0193457	97.10%	95.03%	79.38%

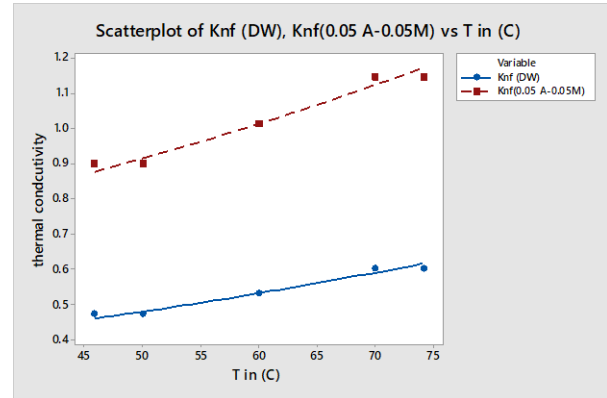


**Figure 2.** Temperature-dependent thermal conductivity of DW and nanofluids.

**Table 4.** Summary of the density regression coefficient model.

S	R-sq	R-sq(adj)	R-sq(pred)
0.0007171	97.06%	94.96%	79.07%

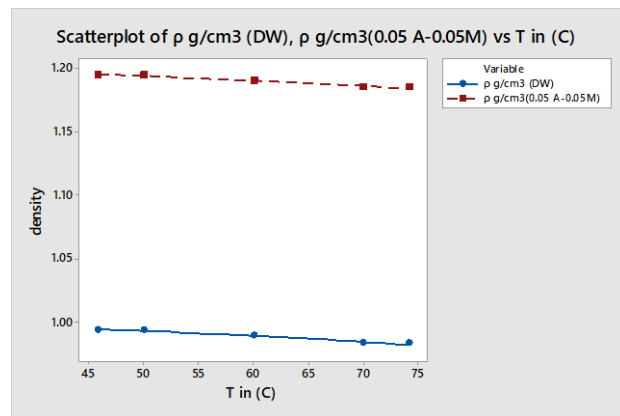


**Figure 3.** displays the DW and nanofluid densities as a function of temperature.

However, due to the lower specific heat of the nanoparticles themselves, the overall specific heat of the nanofluid mixture is only 4179.6 J/kg.k, which is lower than that of the base fluid. Having a clear understanding of the concept of specific heat is essential for comprehending processes related to heat transfer. Nanoparticles have an extraordinary ability to conduct heat because of their distinct qualities. When the substance gets heated, its molecules soak up more energy, causing the nanoparticles to collide and move around. This movement elevates the internal energy and aids in the production of warmth. At a temperature of 70°C, purified water possesses a specific heat of 4359 J/kg.k, whereas the nanofluid exhibits a specific heat of 4000.2 J/kg.k. Consequently, it can be deduced that as the temperature escalates, the specific heat also experiences an upsurge. By studying the various factors that affect how things work together in real-life situations, we can use a mathematical equation Eq. 8 to predict the specific heat of a substance based on experimental data. To give an example, let's think about

nanofluids. When they are at a temperature of 50°C, their ability to hold heat is measured as 3919.5J/kg.k. However, when the temperature increases to 60°C, their specific heat goes up to 3959.7J/kg.k. Table 5 A high value of R<sup>2</sup> (97.14%) indicates that the model fits the data well.

**Table 5.** Regression coefficient of specific heat of nanofluid: A summary of the model

S	R-sq	R-sq(adj)	R-sq(pred)
6.34060	97.14%	95.10%	79.67%

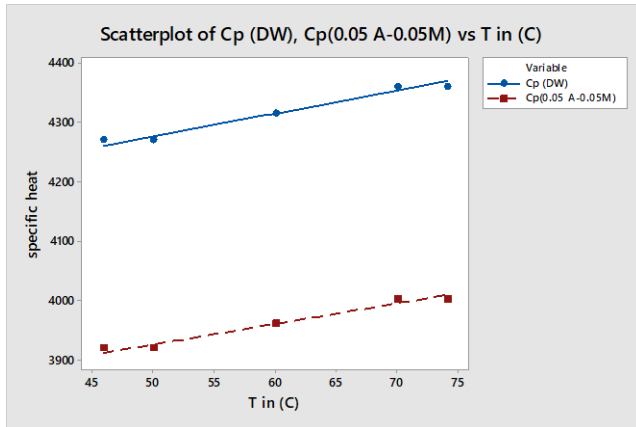


**Figure 4.** demonstrates how DW and nanofluids' specific heat changes with temperature.

$$\begin{aligned} \text{Knf}(0.05 A - 0.05M) = & 0.605 + 0.00333 T \text{ in } ^\circ\text{C}(\text{DW}) - 0.0030 \text{ flow rate (LPM)}(\text{DW}) + 0.000059 T \text{ in } ^\circ\text{C}(\text{DW}) * \\ & T \text{ in } ^\circ\text{C}(\text{DW}) + 0.00030 \text{ flow rate (LPM)}(\text{DW}) * \text{flow rate (LPM)}(\text{DW}) + 0.000000 T \text{ in } ^\circ\text{C}(\text{DW}) * \text{flow rate (LPM)}(\text{DW}) \end{aligned} \tag{6}$$

$$\begin{aligned} \rho\text{g}/\text{cm}^3(0.05 A - 0.05M) = & 1.2014 - 0.000009 T \text{ in (C)}(\text{DW}) + 0.00016 \text{ flow rate (LPM)}(\text{DW}) - 0.000003 T \text{ in (C)}(\text{DW}) \\ & * T \text{ in (C)}(\text{DW}) - 0.000016 \text{ flow rate (LPM)}(\text{DW}) * \text{flow rate (LPM)}(\text{DW}) - 0.000000 T \text{ in (C)}(\text{DW}) * \text{flow rate (LPM)}(\text{DW}) \end{aligned} \tag{7}$$

$$\begin{aligned} \text{Cp}(0.05 A - 0.05M) = & 3752 + 3.46 T \text{ in (C)}(\text{DW}) - 0.0 \text{ flow rate (LPM)}(\text{DW}) - 0.0000 T \text{ in (C)}(\text{DW}) * T \text{ in (C)}(\text{DW}) \\ & + 0.000 \text{ flow rate (LPM)}(\text{DW}) * \text{flow rate (LPM)}(\text{DW}) + 0.000 T \text{ in (C)}(\text{DW}) * \text{flow rate (LPM)}(\text{DW}) \end{aligned} \tag{8}$$

$$\begin{aligned} \mu(0.05A - 0.05M) = & 2.094 - 0.03483 T \text{ in } ^\circ\text{C}(\text{DW}) - 0.0102 \text{ flow rate (LPM)}(\text{DW}) + 0.000203 T \text{ in } ^\circ\text{C}(\text{DW}) * T \text{ in } ^\circ\text{C}(\text{DW}) \\ & + 0.00102 \text{ flow rate (LPM)}(\text{DW}) * \text{flow rate (LPM)}(\text{DW}) - 0.000000 T \text{ in } ^\circ\text{C}(\text{DW}) * \text{flow rate (LPM)}(\text{DW}) \end{aligned} \tag{9}$$

### 7.3. Viscosity

The consistency of nanofluids can change based on the size of the tiny particles, even if they are composed of the same substance. Generally, larger particles tend to result in higher viscosity for nanofluids. However, a few studies have revealed a decline in viscosity as particle size increases. At a temperature of 50°C, Figure 5 illustrates that when nanoparticles are introduced, the nanofluid's viscosity rises. The viscosity of the nanofluid peaks at 0.865 mpa.s, whereas distilled water possesses a viscosity of 0.67 mpa.s. Furthermore, the findings suggest that as temperature rises, viscosity

declines. When the temperature reaches 60°C, the viscosity of the nanofluid is measured to be 0.710 mpa.s.

**Table 6.** Viscosity regression coefficient model summary

S	R-sq	R-sq(adj)	R-sq(pred)
0.0210536	96.68%	94.31%	76.39%

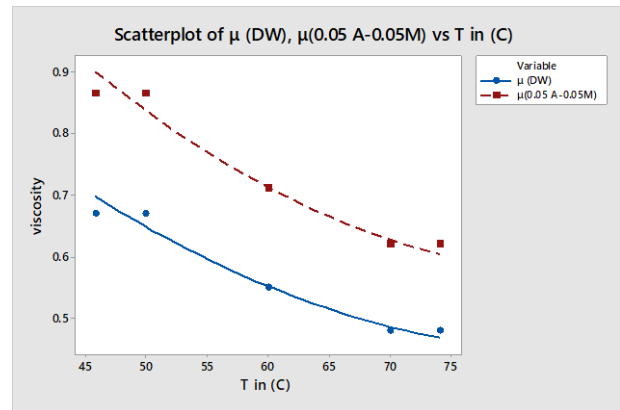


**Figure 5.** demonstrates how DW and nanofluid viscosity changes with temperature.

As the temperature increases to 70°C, the viscosity further drops to 0.620 mpa.s. Our research aligns with previous studies [26-29] and indicates that there is a clear connection between temperature and viscosity in all samples, not just limited to distilled water. As the temperature rises, the viscosity of the nanofluid decreases due to an increase in particle energy and greater distances between molecules. This phenomenon ultimately results in a decrease in intermolecular cuteness [30]. By examining various operational factors and practical parameters, we can employ a mathematical Eq. 9 to predict the viscosity using empirical data. Table 6 shows the high value of

$R^2$  (96.66%), which indicates that the model fits the data well

## 8. Conclusion

The aim of employing hybrid nanofluids consisting of  $Al_2O_3$ , MWCNTs, and DW is to augment the efficiency of vehicle cooling mechanisms. This analysis does preliminary research and explores the heat transmission mechanisms found in automobile radiators. The study's conclusions suggest that adding a nano-suspension system could improve a car's cooling effectiveness. Moreover, it was found that temperature affects the thermal characteristics of nanofluids. More specifically, at higher temperatures, specific heat and thermal conductivity rise considerably relative to DW while density and viscosity decrease...

## Authors' contribution

Each author made an equal contribution to the writing of this article.

## Declaration of competing interest

The writers say they have no competing interests.

## Funding source

There were no special funds for this study.

## REFERENCES

- [1] K. Protocol, United Nations framework convention on climate change, Kyoto Protocol, Kyoto, 19(8) (1997) 1-21.
- [2] K. Yoo, K. Simpson, M. Bell, S. Majkowski, An Engine Coolant Temperature Model and Application for Cooling System Diagnosis, SAE Transactions, 109 (2000) 950-960. <http://www.jstor.org/stable/44634280>
- [3] C.T. Yaw, S. Koh, M. Sandhya, K. Kadirgama, S.K. Tiong, D. Ramasamy, K. Sudhakar, M. Samykan, F. Benedict, C.H. Tan, Heat Transfer Enhancement by Hybrid Nano Additives—Graphene Nanoplatelets/Cellulose Nanocrystal for the Automobile Cooling System (Radiator), Nanomaterials 13(5) (2023) 808. <https://doi.org/10.3390/nano13050808>
- [4] S.O. Giwa, M. Sharifpur, J.P. Meyer, Experimental study of thermo-convection performance of hybrid nanofluids of  $Al_2O_3$ -MWCNT/water in a differentially heated square cavity, International Journal of Heat and Mass Transfer 148 (2020) <https://doi.org/10.1016/j.ijheatmasstransfer.2019.11>
- [5] M. Yasir, A. Hafeez, M. Khan, Thermal conductivity performance in hybrid (SWCNTs-CuO/Ethylene glycol) nanofluid flow: Dual solutions, Ain Shams Engineering Journal 13(5) (2022) 101703. <https://doi.org/10.1016/j.asej.2022.101703>
- [6] M. Arif, P. Kumam, W. Kumam, Z. Mostafa, Heat transfer analysis of radiator using different shaped nanoparticles water-based ternary hybrid nanofluid with applications: A fractional model, Case Studies in Thermal Engineering 31 (2022) 101837. <https://doi.org/10.1016/j.csite.2022.101837>
- [7] D.K. Mandal, N. Biswas, N.K. Manna, D.K. Gayen, R.S.R. Gorla, A.J. Chamkha, Thermo-fluidic transport process in a novel M-shaped cavity packed with non-Darcian porous medium and hybrid nanofluid: Application of artificial neural network (ANN), Physics of Fluids 34(3) (2022) 033608. <https://doi.org/10.1063/5.0082942>
- [8] N.A. Zainal, R. Nazar, K. Naganthran, I. Pop, The impact of thermal radiation on Maxwell hybrid nanofluids in the stagnation region, Nanomaterials 12(7) (2022) 1109. <https://www.mdpi.com/2079-4991/12/7/1109#>
- [9] M.S. Kumar, V. Vasu, Nanofluids Application for Cutting Fluids, Advances in Sustainable Machining and Manufacturing Processes, CRC Press 2022, p. 29.
- [10] M. Javaid, A. Haleem, R.P. Singh, R. Suman, E.S. Gonzalez, Understanding the adoption of Industry 4.0 technologies in improving environmental sustainability, Sustainable Operations and Computers 3 (2022) 203-217. <https://doi.org/10.1016/j.susoc.2022.01.008>
- [11] H.W. Xian, N.A.C. Sidik, R. Saidur, Hybrid nanocoolant for enhanced heat transfer performance in vehicle cooling system, International Communications in Heat and Mass Transfer 133 (2022) 105922. <https://doi.org/10.1016/j.icheatmasstransfer.2022.1>
- [12] H. Nasef, S. Nada, H. Hassan, Integrative passive and active cooling system using PCM and nanofluid for thermal regulation of concentrated photovoltaic solar cells, Energy Conversion and Management 199 (2019) 112065. <https://doi.org/10.1016/j.enconman.2019.112065>
- [13] Y. Huang, X. Xiao, H. Kang, J. Lv, R. Zeng, J. Shen, Thermal management of polymer electrolyte membrane fuel cells: A critical review of heat transfer mechanisms, cooling approaches, and advanced cooling techniques analysis, Energy Conversion and Management 254 (2022) 115221. <https://doi.org/10.1016/j.enconman.2022.115221>
- [14] N.A.C. Sidik, M.N.A.W.M. Yazid, R. Matam, A review on the application of nanofluids in vehicle engine cooling system, International Communications in Heat Mass Transfer, 68 (2015) 85-90. <https://doi.org/10.1016/j.icheatmasstransfer.2015.08.017>
- [15] M. Satar, H. I. Dawood, A comparative study on stability and thermal properties of various nanofluids, Al-Qadisiyah Journal for Engineering Sciences, 14(1) (2021) 41-46. <https://doi.org/10.30772/qjes.v14i1.732>
- [16] S.O. Giwa, M. Sharifpur, J.P. Meyer, Experimental study of thermo-convection performance of hybrid nanofluids of  $Al_2O_3$ -MWCNT/water in a differentially heated square cavity, International Journal of Heat and Mass Transfer 148 (2020) 119072. <https://doi.org/10.1016/j.ijheatmasstransfer.2019.11>
- [17] S.S. Chougule, S.K. Sahu, Comparative study of cooling performance of automobile radiator using  $Al_2O_3$ -water and carbon nanotube-water nanofluid, Journal of Nanotechnology in Engineering Medicine, 5(1) (2014) 010901. <https://doi.org/10.1115/1.4026971>
- [18] Y.A. Cengel, M.A. Boles, M. Kanoğlu, Thermodynamics: an engineering approach, Nine Edition ed., McGraw-hill, New York, 2019.
- [19] [1] R.J. Issa, A Review on Thermophysical Properties and Nusselt Number Behavior of  $Al_2O_3$  Nanofluids in Heat Exchangers, Journal of Thermal Science 30 (2021) 418-431. <https://doi.org/10.1007/s11630-021-1266-1>
- [20] P. Estellé, S. Halelfadl, M. Thierry, Thermal conductivity of CNT water based nanofluids: Experimental trends and models overview, Journal of Thermal Engineering, 1 (2)(2015) 381-390. <https://doi.org/10.18186/jte.92293>
- [21] R. Du, D. Jiang, Y. Wang, Numerical investigation of the effect of nanoparticle diameter and sphericity on the thermal performance of geothermal heat exchanger using nanofluid as heat transfer fluid, Energies, 13 (7)(2020) 1653. <https://doi.org/10.3390/en13071653>
- [22] H.-M. Nieh, T.-P. Teng, C.-C. Yu, Enhanced heat dissipation of a radiator using oxide nano-coolant, International Journal of Thermal Sciences, 77 (2014) 252-261. <https://doi.org/10.1016/j.ijthermalsci.2013.11.008>
- [23] D.R. Ray, D.K. Das, Superior performance of nanofluids in an automotive radiator, Journal of Thermal Science Engineering Applications, 6 (4)(2014) 041002. <https://doi.org/10.1115/1.4027302>
- [24] J.K. Mannekote, S.V. Kailas, K. Venkatesh, N. Kathyayini, Environmentally friendly functional fluids from renewable and sustainable sources-A review, Renewable sustainable energy reviews, 81 (2018) 1787-1801. <https://doi.org/10.1016/j.rser.2017.05.274>
- [25] V. Kumar, J. Sarkar, Particle ratio optimization of  $Al_2O_3$ -MWCNT hybrid nanofluid in minichannel heat sink for best hydrothermal performance, Applied Thermal Engineering 165 (2020) 114546. <https://doi.org/10.1016/j.applthermaleng.2019.114>
- [26] Z. Said, M. Sajid, R. Saidur, G. Mahdiraji, N. Rahim, Evaluating the optical properties of  $TiO_2$  nanofluid for a direct absorption solar collector, Numerical Heat Transfer, Part A: Applications, 67 (9)(2015) 1010-1027. <https://doi.org/10.1080/10407782.2014.955344>
- [27] M. Gupta, V. Singh, S. Kumar, S. Kumar, N. Dilbaghi, Z. Said, Up to date review on the synthesis and thermophysical properties of hybrid nanofluids, Journal of cleaner production, 190 (2018) 169-192. <https://doi.org/10.1016/j.jclepro.2018.04.146>
- [28] M. Elias, I.M. Mahbulul, R. Saidur, M. Sohel, I. Shahrul, S. Khaleduzzaman, S. Sadeghipour, Experimental investigation on the thermo-physical properties of  $Al_2O_3$  nanoparticles suspended in car radiator coolant, International Communications in Heat Mass Transfer, 54 (2014) 48-53. <https://doi.org/10.1016/j.icheatmasstransfer.2014.03.005>
- [29] T.-P. Teng, C.-C. Yu, Heat dissipation performance of MWCNTs nano-coolant for vehicle, Experimental Thermal Fluid Science, 49 (2013) 22-30. <https://doi.org/10.1016/j.exthermflusci.2013.03.007>
- [30] M. Gupta, V. Singh, R. Kumar, Z. Said, A review on thermophysical properties of nanofluids and heat transfer applications, Renewable Sustainable Energy Reviews, 74 (2017) 638-670. <https://doi.org/10.1016/j.rser.2017.02.073>